RETRIEVAL OF AEROSOL MICROPHYSICAL PROPERTIES FROM THE AERONET

PHOTO-POLARIMETRIC MEASUREMENTS

by

Xiaoguang Xu

A DISSERTATION

Presented to the Faculty of

The Graduate College at the University of Nebraska

In Partial Fulfilment of Requirements

For the Degree of Doctor of Philosophy

Major: Earth & Atmospheric Sciences
(Meteorology/Climatology)

Under the Supervision of Professor Jun Wang

Lincoln, Nebraska

May, 2015

Table of Contents

List of Figures

List of Tables

CHAPTER 1

INTRODUCTION

1.1   Background and Motivation

Atmospheric aerosols play a crucial role in the global climate change. They affect earth energy budget directly by scattering and absorbing solar and terrestrial radiation, and indirectly through altering the cloud formation, lifetime, and radiative properties [*Haywood and Boucher*, 2000; *Ramanathan et al.*, 2001]. However, quantification of these effects in the current climate models is fraught with uncertainties. The global average of aerosol effective radiative forcing were estimated to range from –0.1 to –1.9 Wm^{-2} with the best estimate of –0.9 Wm^{-2} [*Boucher et al.*, 2013], indicating that the cooling effects of aerosol might counteract the warming effects of 1.82±0.19 Wm^{-2} caused by the increase of carbon dioxide since the industrial revolution [*Myhre et al.*, 2013]. The climate effects of aerosol particles depend on their geographical distribution, optical properties, and efficiency as cloud condensation nuclei and ice nuclei. Key quantities pertain to the aerosol optical and cloud-forming properties include particle size distribution (PSD), chemical composition, mixing state, and morphology [Boucher et al., 2013]. While the daily aerosol optical depth (AOD) can be well measured from current satellite and ground-based remote sensing instrumentations [e.g., *Holben et al.*, 1998; *Kaufman et al.*, 2002], the accurate quantification of aerosol ERF is in no small part hindered by our limited knowledge about the aerosol PSD and refractive index (describing chemical composition and mixing state).

To fully understand the role of aerosol particles in the global climate change, further development in observations along with retrieval algorithms for these aerosol microphysical properties from different platforms are thus highly needed [*Mishchenko et al.*, 2004], and the focus of this two-part series study is the characterization of aerosol properties from ground-based passive remote sensing.

1.1.1   Previous studies on aerosol microphysical retrievals

There have been continuous efforts in determining aerosol microphysical properties from ground-based measurements of direct and/or diffuse solar radiation since *Ångström* [1929] first suggested an empirical relationship between the spectral dependency of extinction coefficients and the size of aerosol particles. Over thirty years later, *Curcio* [1961] inferred the aerosol PSD from the spectral particulate extinction coefficients in the visible and near-infrared regions. Soon with the effective numerical inversion technique developed by *Phillips* [1962] and *Twomey* [1963] specifically for error-involved optimization, a number of studies explored the use of either spectral attenuations or scattered radiances (in a small range of scattering angles) to determine the aerosol PSD [*Twomey and Howell*, 1967; *Yamamoto and Tanaka*, 1969; *Dave*, 1971; *Grassl*, 1971; *Herman et al.*, 1971; *King et al.*, 1978]. *Shaw* [1979] and *Nakajima et al.* [1983] were among the first studies that have combined optical scattering measurements with spectral extinctions to recover particle size spectrum. *Kaufman et al.* [1994] suggested useful information contained in the sky radiances of larger scattering angles to retrieve the aerosol scattering phase function and PSD. The first operational retrieval algorithm for aerosol microphysical properties was introduced by *Nakajima et al.* [1996], when the multi-band automatic sun- and sky-scanning radiometer was deployed in the AErosol RObotic NETwork, or the AERONET [*Holben et al.*, 1998]. All of above mentioned methods treated aerosol particles as homogeneous

spheres and with refractive index assumed a priori, even though the refractive index can highly impact the optical, especially the scattering characteristics [*Hansen and Travis*, 1974]. *Tanaka et al.* [1982, 1983] developed an inversion library method to estimate the complex refractive index and PSD simultaneously from measurements of scattered radiances polarized in the perpendicular and parallel directions. Another concept for determining refractive index from both direct and diffuse angular radiances was developed by *Wendisch and Von Hoyningen-Huene* [1994] and *Yamasoe et al.* [1998], which were based on the fact that sensitivities of scattered radiances to the PSD and those to the refractive index are dominated on different scattering-angular regions. The current AERONET operational inversion algorithm was developed by *Dubovik and King* [2000], which has heritage from algorithms developed by *King et al.* [1978] and *Nakajima et al.* [1983, 1996] but was implemented for simultaneous retrieval of particle size distribution and complex refractive index with sophisticated inclusion of multiple a priori constraints. *Dubovik et al.* [2002a, 2006] further implemented the spheroids in the particle shape consideration for desert dust in the retrieval, and added fractional volume of non-spherical particles to the inversion products.

1.1.2   The AERONET measurements

With over 400 locations around the word, most AERONET sites are equipped with an automatic sun and sky scanning spectral radiometer, or the CIMEL-318 type SunPhotometer (Figure 1.1a), to routinely measure direct and diffuse solar radiation in various atmospheric window channels [*Holben et al.*, 1998]. As listed in Table 1.1 and illustrated in Figure 1.1, these measurements include direct sun radiances, sky radiance on both the solar almuncantar and pruncipal planes, as well as the optional polarization of sky light on the solar principal plane.
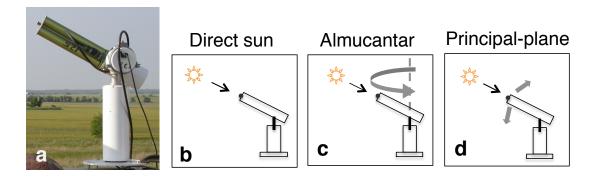
Figure 1.1: A photo of the CIMEL-318 type SunPhotometer and its observational modes.

Direct sun radiances at various atmospheric window channels from the ultra-violet (UV) to near-infrared (NIR) are used to infer the spectral AODs with the Beer-Lambert-Bouguer Law [*Holben et al.*, 1998; *Smirnov et al.*, 2000]. Depending on site-specific instruments, AOT values are typically reported at 7 wavelengths centered at 340 nm, 380 nm, 440 nm, 500 nm, 675 nm, 870 nm, and 1020 nm. Their calibration errors are believed to as small as 0.01 for visible and NIR bands and 0.02 for UV bands.

Sky radiance measurements, which are performed at 440, 670, 870, and 1020-nm bands with full width spectrum at half maximum (FWHM) of 10 nm, are acquired from both solar almucantar and solar principal plane. An almucantar is a series of measurements taken at the viewing angle of the sun for 76 specified relative azimuthal angles (for detail see table 2 of citepholben98). To achieve an enough range of scattering angles, almucantar scans are usually made at an optical air mass of 1.7 or more (corresponding to solar zenith angle larger than about 50°). The principal-plane sequence for each spectrum performs right after almucantar scans. It begins with a sun observation, moves 6°) below the sunray, sweeps up through the sun, and ends at a scattering angle of 150°) or viewing angle achieves horizon, collecting radiances from up to 42 viewing angles. Hereinafter, we will use I_{alm} and I_{ppl} to represent the sky radiances from the solar almucantar and solar principal plane, respectively.

These sky radiance data are used in the current AEROENT operational inversion al-

Table 1.1: Measurement sequences of the CIMEL-318 SunPhotometer.

	Spectra (nm)	Viewing Geometry (°)	Applications
Direct sun	340–1020 340–1640[a]	Target to the sun	AOD, P_w, AE
Almucantar (I_{alm})	440, 675, 870, 1020 (340, 380, 500, 1640)[a]	Azimuth angles relative to Sun: 6, 5, 4.5, 4, 3.5, 3, 2.5, 2, –2, –2.5, –3, –3.5, –4, –4.5, –5, –6, –8, –10, –12, –14, –16, –18, –20, –25, –30, –35, –40, –45, –50, –60, –70, –80, –90, –100, –110, –120, –130, –140, –160, –180 (Duplicate above sequence for a complete counter clockwise rotation to –6)	PSD, m_r, m_i, SSA, phase function
Principal-plane (I_{ppl})	Same as above	Scattering angle from Sun: –6, –5, –4.5, –4, –3.5, –3, –2.5, –2, 2, 2.5, 3, 3.5, 4, 4.5, 5, 6, 8, 10, 12, 14, 16, 18, 20, 25, 30, 35, 40, 45, 50, 60, 70, 80, 90, 100, 110, 120, 130, 140 (negative is below the Sun)	Same as above
Polarization (I_{pp}, $DOLP_{pp}$)	870, (340, 380, 440, 500, 675, 870, 1020, 1640)[a]	Zenith angle on the solar principal plane: –85, –80, –75, –70, –65, –60, –55, –50, –45, –40, –35, –30, –25, –20, –15, –10, –5, 5, 10, 15, 20, 25, 30, 35, 40, 45, 50, 55, 60, 65, 70, 75, 80, 85 (negative is in the antisolar direction)	Not used yet

[a]Additional measurements taken by the newer-generation CIMEL-318DP SunPhotometer.

gorithm [*Dubovik and King*, 2000; *Dubovik et al.*, 2006] (hereafter Dubovik00&06) to derive: (1) the aerosol particle size distribution (PSD) in terms of the aerosol volume (in the atmospheric column) at 22 size bins, (2) the fractional volume of non-spherical particles, and (3) the complex refractive index assumed to be independent of particle size. From those microphysical parameters, the Dubovik00&06 algorithm computes the aerosol single scattering albedo (SSA) and the phase function. Uncertainties in the AERONET inversion products are 15–100% for the bin-based PSD parameters, 0.025–0.05 for real-part refractive index and 0.03 for SSA [*Dubovik et al.*, 2000].

Light polarization measurements are performed optionally over many sites. They are measured by the SunPhotometer with three polarizers placed 60° between each axial direction. The total radiance is derived by

$$I_{pp} = \frac{2}{3}\left(I_1 + I_2 + I_3\right), \tag{1.1}$$

where I_1, I_2, and I_3 are radiance with these three polarizers, respectively. The degree of linear polarization (DOLP) of skylight is inferred by

$$\text{DOLP}_{\text{pp}} = \frac{2(I_1^2 + I_2^2 + I_3^2 - I_1I_2 - I_2I_3 - I_1I_3)^{(1/2)}}{I_1 + I_2 + I_3}.$$

(1.2)

It should be noted that we prefer to use DOLP_{pp} instead of polarized radiance in our inversion, since as a relative quantity it is more accurate. Polarization measurements are made every hour (right after principal plane scans) at 870 nm in the principal plane at $5°$ increments between viewing zenith angle of $-85°$ and $+85°$. These measurements are optional depending on the instrument version and configuration, and are currently available mostly over European and African stations. Recently, multi-spectral polarizations have also been taken with a newer-generation SunPhotometer (CIMEL CE318-DP) at some sites [*Li et al.*, 2009] and the UAE[2] fields campaign [*Reid et al.*, 2008]. Here we focus our study on using multi-spectral polarizations for the inversion of aerosol parameters.

1.1.3 Challenges and opportunities

While the AERONET AOD and other inversion products have been widely used to study the climatology of aerosol optical properties [*Dubovik et al.*, 2002b; *Levy et al.*, 2007a] and for the development and validation of aerosol retrieval algorithms for satellite sensors such as the Moderate Resolution Imaging Spectrometer (MODIS) [*Kaufman et al.*, 1997; *Remer et al.*, 2005; *Levy et al.*, 2007b, 2010; *Wang et al.*, 2010] and the Multi-angle Imaging SpectroRadiometer (MISR) [*Diner et al.*, 1998; *Kahn et al.*, 2010], the AERONET operational algorithm also faces: (i) challenges in evaluation of aerosol data either retrieved from newer-generation satellite sensors or simulated from chemistry transport models, and (ii) opportunities to improve the retrieval through the use of multi-spectral polarization measurements that are now available at a few sites and will be made available at more sites as

part of the AERONET future research development (http://aeronet.gsfc.nasa.gov).
These challenges and opportunities, as further described below, are also the motivation for
us to develop a new research algorithm.

The first challenge is that newer-generation satellite sensors are expected to offer aerosol
microphysical products with accuracy that is equivalent to, if not higher than, that of the
current AERONET microphysical products. For instance, the Aerosol Polarimetry Sensor
(APS) for the NASA Glory mission, through measuring the first three Stokes vector elements
simultaneously from 250 viewing angles at nine spectral bands (410, 443, 556, 670, 865,
910, 1370, 1610, and 2200 nm), was designed to retrieve aerosol effective radius (r_{eff}),
effective variance (v_{eff}), and spectral complex index of refraction for both fine and coarse
modes [*Mishchenko et al.*, 2007]. While no actual product is available because of the failure
of Glory launch, several case studies with the APS's prototype airborne sensor, RSP (the
Remote Sensing Polarimeter), demonstrated feasibility of APS algorithm [*Chowdhary et al.*,
2002, 2005; *Mishchenko et al.*, 2004; *Waquet et al.*, 2009]. At least in the case of spherical
particles, the accuracy of APS's bi-modal aerosol products was expected to be 10% for r_{eff},
40% for v_{eff}, 0.02 for m_{r}, and 0.03 for the SSA (ω_{A}) [*Mishchenko et al.*, 2007]. Some of
these accuracy expectations are unlikely to be matched by existing ground-based and in
situ instruments, including those at the AERONET sites. Moreover, the current AERONET
retrieval of the refractive index and the ω_{A} are not recommended to use when the 440-nm
AOD is lower than 0.4 [*Holben et al.*, 2006] due to expected limited accuracy identified in
the detailed sensitivity study by [*Dubovik et al.*, 2000].

The second challenge is associated with the inconsistency in assumptions of PSD that
exists between current AERONET inversion products and satellite retrievals on the one
hand, as well as the aerosol models used by climate models on the other hand. Specifically,
the Dubovik00&06 algorithm retrieves the aerosol PSD on in 22 discrete size bins. In
contrast, a continuous PSD function (e.g., lognormal) is usually assumed in satellite retrieval

algorithms, such as those for APS/RSP [*Mishchenko et al.*, 2007; *Waquet et al.*, 2009] and the POLDER/PARASOL algorithm [*Hasekamp et al.*, 2011]. Also, aerosol microphysical properties are usually calculated with continuous PSD assumptions in many chemistry transport models, such as GEOS-Chem [*Drury et al.*, 2010; *Wang et al.*, 2010] and the GOCART model [*Chin et al.*, 2002]. Clearly, the actual aerosol PSD is never a perfect lognormal distribution, but neither it is discrete. At least from the scattering perspective, the aerosol PSD can be well characterized with an effective radius r_{eff} and an effective variance v_{eff}, while the specific function of the PSD is shown to be much less important [*Hansen and Travis*, 1974]. In other words, since the retrieval is based on the information content in the particle optical scattering, the most relevant size parameters, regardless of the PSD shape, should be r_{eff} and v_{eff}, at least for spherical particles.

The third challenge is that the assumption of a size-independent refractive index (and SSA) in Dubovik00&06 is not in line with the majority of counterpart satellite retrieval algorithms [e.g., *Mishchenko et al.*, 2007; *Hasekamp et al.*, 2011; *Martonchik et al.*, 2009], which often uses different refractive indices for various individual aerosol modes. In many cases, tropospheric aerosol is a mixture of modes with substantially different refractive indices. For example, smoke from biomass burning can be mixed with mineral dust over western coastal North Africa [*Yang et al.*, 2013]. Furthermore, the assumption of size-independent refractive index can lead to errors in the retrieval of the size distributions when the refractive indices for fine- and coarse-mode aerosols differ substantially [*Dubovik et al.*, 2000; *Chowdhary et al.*, 2001]. Thus, a mode-resolved parameterization of the refractive index in an aerosol retrieval algorithm not only can facilitate the validation of satellite products and chemistry transport models, but also is expected to improve the accuracy of PSD and SSA retrievals for each mode. [*Dubovik et al.*, 2000] have tested the possibility of retrieving separated refractive indices of fine and coarse modes, however, they concluded that the retrieval of bi-modal refractive indices is essentially non-unique due to limited

information in the AERONET radiance-only observations.

Therefore, this work aims to developing an algorithm to retrieve the aerosol microphysical properties of both fine and coarse aerosol modes, which embraces the future opportunities of deploying polarization measurements through AERONET, and ameliorates the aforementioned limitations in the Dubovik00&06 algorithm by incorporating both radiance and polarization data. Polarization measurements contain valuable information on aerosol microphysical properties [*Mishchenko and Travis*, 1997], as the polarization of the scattered light is highly sensitive to aerosol size and refractive index [*Hansen and Travis*, 1974; *Mishchenko et al.*, 2002]. We note, however, their conclusions were based on consideration of spherical aerosol particles and were primarily from a theoretical point of view. In contrast, the studies by *Dubovik et al.* [2006] and *Deuzé et al.* [1993, 2001] revealed serious limitation of polarimetric retrieval of the properties for coarse, especially non-spherical aerosols. Moreover, *Dubovik et al.* [2006] have shown that while the polarimetic observation of fine particles and large spheres are highly sensitive to real part of refractive index, even they have non-negligible sensitivity to particle shape. Therefore, adding polarization measurements to the inversion has great potential to improve the accuracy of AERONET microphysical retrievals, provided that the difficulty of representing aerosol particle shapes is recognized or adequately addressed. In these regards, most of the past efforts seem to suggest clear improvements in characterization of fine mode aerosol using polarimetric observations. For example, *Li et al.* [2009], based upon the Dubovik00&06 algorithm, demonstrated the possibility to reduce errors in the fine-mode size distribution, real part of the refractive index, and particle shape parameters.

1.2 Research Goals and Thesis Outline

As discussed above, this dissertation seeks to contribute to an improved research algorithm to retrieval aerosol micriphysical properties from AERONET measurements of light radiance and polarization, with emphasis on elucidating the potentially important role of polarization measurements. It does so by pursuing three following spcifci objectives:

1. *Develop ground-based inversion algorithms for the retrieval of r_{eff}, v_{eff}, m_r, and m_i from a combined use of direct solar radiance, skylight radiance and skylight linear polarization measurements from AERONET.*

2. *Perform a sensitivity study and error budgeting exercise to characterize retrieval accuracy and error sources.*
   By doing so, we can answer the questions:

3. *Perform ground-based retrievals using available AERONET polarimetric measurements.*

CHAPTER 2

MODEL DEVELOPMENTS

2.1   Introduction

The radiation fields—radiance and the state of polarization—measured by the AERONET SunPhotometer are the outcome of the interations of solar radiation with various physical processes including the absorption and scattering by atmospheric molecules, aerosols and clouds, as well the reflection and absorption by underlying surface. The radiance and polarization of light at any wavelength can be represented by a Stokes column vector **I** having four elements [*Hansen and Travis*, 1974]:

$$\mathbf{I} = [I, Q, U, V]^T, \tag{2.1}$$

where I is the total intensity (or radiance), Q and U describe the state of linear polarization, V describes the state of circular polarization, and T indicates a transposed matrix. It should be noted that all radiation fields and optical parameters used in this paper are functions of the light wavelength λ. For simplicity, however, we omit λ in all formulas. The degree of linear polarization (DOLP) is defined by

$$\text{DOLP} = \frac{\sqrt{Q^2 + U^2}}{I}. \tag{2.2}$$

In the solar principal plane, U is negligibly small and the above formula becomes DOLP $= -Q/I$. Let $\mathbf{I}_0 = [I_0, 0, 0, 0]^T$ denote the Stokes vector for incident Solar radiation at the top of the atmosphere (TOA) from the direction (θ_0, ϕ_0), where θ_0 and ϕ_0 are the incident solar zenith and azimuth angles, respectively. For a plane-parallel atmosphere bounded below by a reflective surface, the vector radiative transfer equation in the medium for the specific intensity column vector $\mathbf{I}$ of light propagating in the viewing direction (θ, ϕ) can be written [*Hovenier et al.*, 2004; *Mishchenko et al.*, 2002]:

$$\mu \frac{\partial \mathbf{I}(\tau, \mu, \phi)}{\partial \tau} = \mathbf{I}(\tau, \mu, \phi) - \mathbf{J}(\tau, \mu, \phi; \mu_0, \phi_0) \tag{2.3}$$

$$\begin{aligned}
\mathbf{J}(\tau, \mu, \phi; \mu_0, \phi_0) &= \frac{\omega}{4\pi} \int_{-1}^{1} \int_{0}^{2\pi} \mathbf{P}(\tau, \mu, \mu_0, \phi - \phi_0) \mathbf{I}(\tau, \mu_0, \phi_0) d\phi_0 d\mu_0 \\
&+ \frac{\omega}{4\pi} \mathbf{P}(\tau, \mu, \mu_0, \phi - \phi_0) \mathbf{I}_0 \exp(-\tau/\mu_0)
\end{aligned} \tag{2.4}$$

Here, τ is the extinction optical depth measured from TOA, μ and μ_0 are cosines of θ and θ_0, respectively, ω is the SSA and $\mathbf{P}$ is the phase matrix. The first term in equation (2.3) represents multiple scattering contributions, while the second indicates scattered light from the direct solar beam.

Parameters required to solve the above radiative transfer equation are τ, ω, and $\mathbf{P}(\Theta)$ for the atmosphere, and the reflectance matrix $\mathbf{R}_s(\tau, \mu, \phi; \mu_0, \phi_0)$ of the underlying surface. Considering a cloud-free atmosphere, the solar radiation is attenuated by molecular scattering, gaseous absorption, and aerosol scattering and absorption. For a given layer, we have

$$\tau = \tau_A + \tau_R + \tau_G \tag{2.5}$$

$$\omega = \frac{\tau_A \omega_A + \tau_R}{\tau} \tag{2.6}$$

$$\mathbf{P}(\Theta) = \mathbf{P}_A(\Theta) \frac{\tau_A \omega_A}{\tau_A \omega_A + \tau_R} + \mathbf{P}_R(\Theta) \frac{\tau_R}{\tau_A \omega_A + \tau_R} \tag{2.7}$$

where τ_A, τ_R, and τ_G are optical depth, respectively, by aerosol extinction, Rayleigh scattering of air density fluctuations, and gaseous absorption. ω_A is the SSA of aerosol, and $\mathbf{P}_A(\Theta)$ and $\mathbf{P}_R(\Theta)$ are, respectively, the aerosol and Rayleigh phase matrices as functions of the scattering angle Θ. The forward modeling of radiance/polarization measurements thus requires knowledge of single scattering properties for aerosols and air density fluctuations, absorption of trace gases, and reflectance/polarization by surface.

2.2 The UNL-VRTM

2.2.1 Surface representations

2.2.2 Molecular scattering and absorption

2.2.3 Aerosol single scattering

2.2.4 Radiative transfer

2.2.5 Capability of calculating Jacobians

2.3 Model Benchmarking and Verifications

CHAPTER 3

INVERSION ALGORITHM

3.1 General sturcture

Basic formulation of inverse problem; sturcture of the algorithm.

3.2 Combine a priori and smoothness constraints

3.3 Statistical optimized inversion

3.4 Retrieval Error Characertization

3.5 Qaulity Control of Measurements

CHAPTER 4

INFORMATION CONTENT ANALYSIS

4.1   Introduction

4.2   Inversion and Information Theories

4.2.1   Inverse problem and error characterization

4.3   Experiment Design

4.4   Results

4.4.1   Error-normalized (EN) Jacobian matrix

4.4.2   Information content and retrieval error

4.4.2.1   Aerosol PSD

4.4.2.2   Refractive indices

4.4.2.3   Single scattering albedo

To be filled . . .

4.5   Sensitivity of retrieval error to AOD and fmf

To be filled . . .

4.6   Summary

To be filled . . .

CHAPTER 5

CASE DEMONSTRATIONS

5.1   Selected case and the a priori characterization

5.2   Fitting Residuals

5.3   Retrieved Aerosol Properties

5.4   Improvement over Radiance-Only Retrievals

5.5   Summary

CHAPTER 6

SUMMARY AND OUTLOOK

6.1   Summary of the Dissertation

6.2   Main Conclusions of This Work

6.3   Outlook and Future Work

APPENDIX A

ABBREVIATIONS AND ACRONYMS

APPENDIX B

SYMBOLS

REFERENCES

Boucher, O., et al. (2013), *Clouds and Aerosols. In Climate Change 2013: The Physical Science Basis. Contribution of Working Group I to the Fifth Assessment Report of the Intergovernmental Panel on Climate Change [Stocker T.F., et al. (eds.)]*, p. 571–658, Cambridge University Press, Cambridge, United Kingdom and New York, NY, USA. 1.1

Chin, M., et al. (2002), Tropospheric aerosol optical thickness from the gocart model and comparisons with satellite and sun photometer measurements, *Journal of the Atmospheric Sciences*, *59*(3), 461–483. 1.1.3

Chowdhary, J., B. Cairns, M. Mishchenko, and L. Travis (2001), Retrieval of aerosol properties over the ocean using multispectral and multiangle photopolarimetric measurements from the research scanning polarimeter, *Geophysical Research Letters*, *28*(2), 243–246. 1.1.3

Chowdhary, J., B. Cairns, and L. D. Travis (2002), Case studies of aerosol retrievals over the ocean from multiangle, multispectral photopolarimetric remote sensing data, *Journal of the Atmospheric Sciences*, *59*(3), 383–397. 1.1.3

Chowdhary, J., B. Cairns, M. I. Mishchenko, P. V. Hobbs, G. F. Cota, J. Redemann, K. Rutledge, B. N. Holben, and E. Russell (2005), Retrieval of aerosol scattering and absorption properties from photopolarimetric observations over the ocean during the clams experiment, *Journal of the Atmospheric Sciences*, *62*(4), 1093–1117. 1.1.3

Curcio, J. (1961), Evaluation of atmospheric aerosol particle size distribution from scattering measurements in the visible and infrared, *Journal of the Optical Society of America*, *51*(5), 548–551. 1.1.1

Dave, J. V. (1971), Determination of size distribution of spherical polydispersions using scattered radiation data, *Applied Optics*, *10*(9), 2035–2044. 1.1.1

Deuzé, J. L., F. M. Bréon, P. Y. Deschamps, C. Devaux, M. Herman, A. Podaire, and J. L. Roujean (1993), Analysis of the polder (polarization and directionality of earth's reflectances) airborne instrument observations over land surfaces, *Remote Sensing of Environment*, *45*(2), 137–154. 1.1.3

Deuzé, J. L., et al. (2001), Remote sensing of aerosols over land surfaces from polder-adeos-1 polarized measurements, *Journal of Geophysical Research: Atmospheres*, *106*(D5), 4913–4926. 1.1.3

Diner, D. J., et al. (1998), Multi-angle imaging spectroradiometer (misr) instrument description and experiment overview, *Geoscience and Remote Sensing, IEEE Transactions on*, *36*(4), 1072–1087. 1.1.3

Drury, E., et al. (2010), Synthesis of satellite (modis), aircraft (icartt), and surface (improve, epa-aqs, aeronet) aerosol observations over eastern north america to improve modis aerosol retrievals and constrain surface aerosol concentrations and sources, *J. Geophys. Res.*, *115*(D14), D14,204. 1.1.3

Dubovik, O., and M. D. King (2000), A flexible inversion algorithm for retrieval of aerosol optical properties from sun and sky radiance measurements, *J. Geophys. Res.*, *105*(D16), 20,673–20,696. 1.1.1, 1.1.2

Dubovik, O., A. Smirnov, B. N. Holben, M. D. King, Y. J. Kaufman, T. F. Eck, and I. Slutsker (2000), Accuracy assessments of aerosol optical properties retrieved from aerosol robotic network (aeronet) sun and sky radiance measurements, *Journal of Geophysical Research*, *105*(D8), 9791–9806. 1.1.2, 1.1.3

Dubovik, O., B. N. Holben, T. Lapyonok, A. Sinyuk, M. I. Mishchenko, P. Yang, and I. Slutsker (2002a), Non-spherical aerosol retrieval method employing light scattering by spheroids, *Geophysical Research Letters*, *29*(10). 1.1.1

Dubovik, O., B. Holben, T. F. Eck, A. Smirnov, Y. J. Kaufman, M. D. King, D. Tanre, and I. Slutsker (2002b), Variability of absorption and optical properties of key aerosol types observed in worldwide locations, *Journal of the Atmospheric Sciences*, *59*(3), 590–608. 1.1.3

Dubovik, O., et al. (2006), Application of spheroid models to account for aerosol particle nonsphericity in remote sensing of desert dust, *Journal of Geophysical Research: Atmospheres*, *111*, D11,208. 1.1.1, 1.1.2, 1.1.3

Grassl, H. (1971), Determination of aerosol size distributions from spectral attenuation measurements, *Applied Optics*, *10*(11), 2534–2538. 1.1.1

Hansen, J. E., and L. D. Travis (1974), Light scattering in planetary atmospheres, *Space Sci. Rev.*, *16*, 572–610. 1.1.1, 1.1.3, 2.1

Hasekamp, O. P., P. Litvinov, and A. Butz (2011), Aerosol properties over the ocean from parasol multiangle photopolarimetric measurements, *Journal of Geophysical Research: Atmospheres*, *116*(D14), D14,204. 1.1.3

Haywood, J., and O. Boucher (2000), Estimates of the direct and indirect radiative forcing due to tropospheric aerosols: A review, *Rev. Geophys.*, *38*(4), 513–543. 1.1

Herman, B. M., S. R. Browning, and J. A. Reagan (1971), Determination of aerosol size distributions from lidar measurements, *Journal of the Atmospheric Sciences*, *28*(5), 763–771. 1.1.1

Holben, B. N., et al. (1998), Aeronet - a federated instrument network and data archive for aerosol characterization, *Remote Sensing of Environment*, *66*(1), 1–16. 1.1, 1.1.1, 1.1.2

Holben, B. N., T. F. Eck, I. Slutsker, A. Smirnov, A. Sinyuk, J. Schafer, D. Giles, and O. Dubovik (2006), Aeronet's version 2.0 quality assurance criteria, *Proc. SPIE 6408, Remote Sensing of the Atmosphere and Clouds*, *64080Q*, 10.1117/12.706524. 1.1.3

Hovenier, J., C. v. d. Mee, and H. Domke (2004), *Transfer Of Polarized Light In Planetary Atmospheres*, 258 pp., Kluwer Academic Publishers, Dordrecht, The Netherlands. 2.1

Kahn, R. A., B. J. Gaitley, M. J. Garay, D. J. Diner, T. F. Eck, A. Smirnov, and B. N. Holben (2010), Multiangle imaging spectroradiometer global aerosol product assessment by comparison with the aerosol robotic network, *J. Geophys. Res.*, *115*(D23), D23,209. 1.1.3

Kaufman, Y. J., A. Gitelson, A. Karnieli, E. Ganor, R. S. Fraser, T. Nakajima, S. Mattoo, and B. N. Holben (1994), Size distribution and scattering phase function of aerosol particles retrieved from sky brightness measurements, *Journal of Geophysical Research: Atmospheres*, *99*(D5), 10,341–10,356. 1.1.1

Kaufman, Y. J., D. Tanré, L. A. Remer, E. F. Vermote, A. Chu, and B. N. Holben (1997), Operational remote sensing of tropospheric aerosol over land from eos moderate resolution

imaging spectroradiometer, *Journal of Geophysical Research: Atmospheres*, *102*(D14), 17,051–17,067. 1.1.3

Kaufman, Y. J., D. Tanre, and O. Boucher (2002), A satellite view of aerosols in the climate system, *Nature*, *419*, 215 – 223. 1.1

King, M. D., D. M. Byrne, B. M. Herman, and J. A. Reagan (1978), Aerosol size distributions obtained by inversions of spectral optical depth measurements, *Journal of the Atmospheric Sciences*, *35*(11), 2153–2167. 1.1.1

Levy, R. C., L. A. Remer, and O. Dubovik (2007a), Global aerosol optical properties and application to moderate resolution imaging spectroradiometer aerosol retrieval over land, *Journal of Geophysical Research: Atmospheres*, *112*(D13), D13,210. 1.1.3

Levy, R. C., L. A. Remer, S. Mattoo, E. F. Vermote, and Y. J. Kaufman (2007b), Second-generation operational algorithm: Retrieval of aerosol properties over land from inversion of moderate resolution imaging spectroradiometer spectral reflectance, *J. Geophys. Res.*, *112*(D13), D13,211. 1.1.3

Levy, R. C., L. A. Remer, R. G. Kleidman, S. Mattoo, C. Ichoku, R. Kahn, and T. F. Eck (2010), Global evaluation of the collection 5 modis dark-target aerosol products over land, *Atmos. Chem. Phys.*, *10*(21), 10,399–10,420, aCP. 1.1.3

Li, Z., et al. (2009), Improvements for ground-based remote sensing of atmospheric aerosol properties by additional polarimetric measurements, *Journal of Quantitative Spectroscopy and Radiative Transfer*, *110*(17), 1954–1961. 1.1.2, 1.1.3

Martonchik, J. V., R. A. Kahn, and D. J. Diner (2009), *Retrieval of aerosol properties over land using MISR observations*, Springer, Berlin. 1.1.3

Mishchenko, M. I., and L. D. Travis (1997), Satellite retrieval of aerosol properties over the ocean using polarization as well as intensity of reflected sunlight, *J. Geophys. Res.*, *102*(D14), 16,989–17,013. 1.1.3

Mishchenko, M. I., L. D. Travis, and A. A. Lacis (2002), *Scattering, Absorption, and Emission of Light by Small Particles*, Cambridge University Press, Cambridge, UK. 1.1.3, 2.1

Mishchenko, M. I., B. Cairns, J. E. Hansen, L. D. Travis, R. Burg, Y. J. Kaufman, J. Vanderlei Martins, and E. P. Shettle (2004), Monitoring of aerosol forcing of climate from space: analysis of measurement requirements, *Journal of Quantitative Spectroscopy and Radiative Transfer*, *88*(1-3), 149–161. 1.1, 1.1.3

Mishchenko, M. I., et al. (2007), Accurate monitoring of terrestrial aerosols and total solar irradiance: Introducing the glory mission, *Bulletin of the American Meteorological Society*, *88*(5), 677–691. 1.1.3

Myhre, G., et al. (2013), *Anthropogenic and Natural Radiative Forcing. In Climate Change 2013: The Physical Science Basis. Contribution of Working Group I to the Fifth Assessment Report of the Intergovernmental Panel on Climate Change [Stocker T.F., et al. (eds.)]*, book section 8, p. 659–740, Cambridge University Press, Cambridge, United Kingdom and New York, NY, USA. 1.1

Nakajima, T., M. Tanaka, and T. Yamauchi (1983), Retrieval of the optical properties of aerosols from aureole and extinction data, *Applied Optics*, *22*(19), 2951–2959. 1.1.1

Nakajima, T., G. Tonna, R. Rao, P. Boi, Y. Kaufman, and B. Holben (1996), Use of sky brightness measurements from ground for remote sensing of particulate polydispersions, *Applied Optics*, *35*(15), 2672–2686. 1.1.1

Phillips, D. L. (1962), A technique for the numerical solution of certain integral equations of the first kind, *J. ACM*, *9*(1), 84–97. 1.1.1

Ramanathan, V., P. J. Crutzen, J. T. Kiehl, and D. Rosenfeld (2001), Aerosols, climate, and the hydrological cycle, *Science*, *294*(5549), 2119–2124. 1.1

Reid, J. S., et al. (2008), An overview of uae2 flight operations: Observations of summertime atmospheric thermodynamic and aerosol profiles of the southern arabian gulf, *Journal of Geophysical Research: Atmospheres*, *113*(D14), D14,213. 1.1.2

Remer, L. A., et al. (2005), The modis aerosol algorithm, products, and validation, *Journal of the Atmospheric Sciences*, *62*(4), 947–973. 1.1.3

Shaw, G. E. (1979), Inversion of optical scattering and spectral extinction measurements to recover aerosol size spectra, *Applied Optics*, *18*(7), 988–993. 1.1.1

Smirnov, A., B. N. Holben, T. F. Eck, O. Dubovik, and I. Slutsker (2000), Cloud-screening and quality control algorithms for the aeronet database, *Remote Sensing of Environment*, *73*(3), 337–349. 1.1.2

Tanaka, M., T. Nakajima, and T. Takamura (1982), Simultaneous determination of complex refractive index and size distribution of airborne and water-suspended particles from light scattering measurements, *Meteorological Society of Japan Journal*, *60*, 1259–1272. 1.1.1

Tanaka, M., T. Takamura, and T. Nakajima (1983), Refractive index and size distribution of aerosols as estimated from light scattering measurements, *Journal of Climate and Applied Meteorology*, *22*(7), 1253–1261. 1.1.1

Twomey, S. (1963), On the numerical solution of fredholm integral equations of the first kind by the inversion of the linear system produced by quadrature, *J. ACM*, *10*(1), 97–101. 1.1.1

Twomey, S., and H. B. Howell (1967), Some aspects of the optical estimation of microstructure in fog and cloud, *Applied Optics*, *6*(12), 2125–2131. 1.1.1

Wang, J., X. Xu, R. Spurr, Y. Wang, and E. Drury (2010), Improved algorithm for modis satellite retrievals of aerosol optical thickness over land in dusty atmosphere: Implications for air quality monitoring in china, *Remote Sensing of Environment*, *114*(11), 2575–2583, doi: DOI: 10.1016/j.rse.2010.05.034. 1.1.3

Waquet, F., B. Cairns, K. Knobelspiesse, J. Chowdhary, L. D. Travis, B. Schmid, and M. I. Mishchenko (2009), Polarimetric remote sensing of aerosols over land, *J. Geophys. Res.*, *114*(D1), D01,206. 1.1.3

Wendisch, M., and W. Von Hoyningen-Huene (1994), Possibility of refractive index determination of atmospheric aerosol particles by ground-based solar extinction and scattering measurements, *Atmospheric Environment*, *28*(5), 785–792. 1.1.1

Yamamoto, G., and M. Tanaka (1969), Determination of aerosol size distribution from spectral attenuation measurements, *Applied Optics*, *8*(2), 447–453. 1.1.1

Yamasoe, M. A., Y. J. Kaufman, O. Dubovik, L. A. Remer, B. N. Holben, and P. Artaxo (1998), Retrieval of the real part of the refractive index of smoke particles from sun/sky measurements during scar-b, *Journal of Geophysical Research: Atmospheres*, *103*(D24), 31,893–31,902. 1.1.1

Yang, Z., J. Wang, C. Ichoku, E. Hyer, and J. Zeng (2013), Mesoscale modeling and satellite observation of transport and mixing of smoke and dust particles over northern sub-saharan african region, *Journal of Geophysical Research: Atmospheres*, *118*(21), 12,139–12,157. 1.1.3

Ångström, A. (1929), On the atmospheric transmission of sun radiation and on dust in the air, *Geografiska Annaler*, *11*, 156–166. 1.1.1

LIST OF PUBLICATIONS

List my publication here